Evaluation of GNSS Pulsed Interference Mitigation Techniques Accounting for Signal Conditioning

Daniele Borio[1], Eduardo Cano[1] *Member, IEEE*

Abstract

Pulsed interference can severely degrade the performance of a Global Navigation Satellite System (GNSS) receiver. For this reason, several mitigation techniques have been developed for reducing the impact of disturbing signals. Among the different pulse interference mitigation techniques, Interference Cancellation (IC) and Pulse Blanking (PB) have received particular attention: the former for its optimality in the absence of quantization, the latter for its simplicity and effectiveness. In this paper, IC and PB are assessed in the presence of signal conditioning and the impact of parameters such as the number of bits used for quantization and the front-end Automatic Gain Control (AGC) gain is analyzed. The theoretical analysis is supported and complemented by Monte Carlo simulation results, which show that signal conditioning plays a fundamental role for choosing the most appropriate interference mitigation technique.

Index Terms

Blanking, Global Navigation Satellite Systems, GNSS, Interference Cancellation, IC, Pseudolites, Pulse Interference

I. Introduction

In the last decade, the impact of pulse interference and its mitigation have been the focus of intense research activities (Grabowski and Hegarty; 2002; Hegarty et al.; 2000; Madhani et al.; 2003; Paonni et al.; 2010). Such interest is justified by the allocation of the L5/E5 band

1) Institute for the Protection and Security of Citizen (IPSC), Joint Research Centre, Ispra (VA), Italy. Email: daniele.borio@ieee.org, eduardo.cano-pons@ext.jrc.ec.europa.eu

for Global Navigation Satellite System (GNSS) transmission and the proposed use of pulsed pseudolite signals. In the L5/E5 band, Distance Measuring Equipment (DME) signals are used for landing applications whereas it has been proposed that, for compatibility reasons, some pseudolites could broadcast in the GNSS bands. Both signals are forms of pulsed interference.

The impact of pulsed interference on non-participating receivers, i.e., receivers not implementing any forms of mitigation, has been intensively studied (Borio and Fortuny; 2010; Borio et al.; 2011b; Cobb; 1997) and several models have been developed to predict receiver losses. In addition to this, it has been shown (Gao; 2007; Madhani et al.; 2003; Nava and Scarafia; 2006) that mitigation techniques can significantly reduce the impact of pulsed interference.

Pulsed interference mitigation techniques can be broadly classified as Interference Cancellation (IC)(Madhani et al.; 2003), Pulse Blanking (PB) (Grabowski and Hegarty; 2002; Hegarty et al.; 2000) and Time Frequency (TF) excision (Gao; 2007; Paonni et al.; 2010). IC techniques reconstruct the interference components and remove them from the received signal whereas PB consists of zeroing the corrupted samples by an interference component. Finally, TF excision techniques at first project the one-dimensional time signal over a two-dimensional space where the interference pulse should assume a more compact representation. The interference is then excised and the time domain signal is finally reconstructed. Although these techniques have been the focus of several research works, all the analysis have been conducted by neglecting the impact of quantization and signal conditioning. More specifically, it has always been assumed that interference and useful signals were represented by using an infinite number of bits. Even the most recent results (Soualle et al.; 2011) on PB neglected quantization effects and experimental results were also provided using Analog-to-Digital Converters (ADCs) with at least 8 bits (Madhani et al.; 2003). This is a strong assumption since most of current GNSS receivers operate with a limited number of bits (1 to 3 bits).

In this paper, IC and PB are analyzed and characterized by accounting for signal conditioning. It is shown that IC is the optimal mitigation technique when an infinite number of bits are available. However, its performance degrades as the number of bits decreases. In the limit case when a single bit is used, IC is no longer the most effective mitigation technique since it is not possible to recover the useful signal even if the interference component is removed. In this scenario, PB should be adopted, also because of its reduced computational load. The considered mitigation techniques are characterized theoretically and experimentally taking into

account quantization and the effect of the Automatic Gain Control (AGC). More specifically, a theoretical model, accounting for the number of bits used for quantization and the AGC gain, is developed for PB. This model is then used for the selection of the optimum parameters that minimize the quantization loss. This analysis is new and provides useful criteria for the selection of pulsed interference mitigation techniques.

The remainder of this paper is organized as follows. In Section II, the signal and system models adopted in the paper are briefly described. Specific emphasis is devoted to signal conditioning and quantization. In Section III, the aforementioned mitigation techniques are described and their optimality, under specific operating conditions, is briefly discussed. Theoretical results relative to the expected signal loss are also presented. Simulation results supporting the validity of the theoretical findings are shown in Section IV. Conclusions are finally drawn in Section V.

II. Signal and System Model

The signal at the input of a GNSS receiver in a one-path additive Gaussian channel and in the presence of pulsed interference can be modeled as

$$r(t) = \sum_{l=0}^{L-1} y_l(t) + i(t) + \eta(t) \tag{1}$$

which is the sum of L useful signals transmitted by L different satellites, a pulsed interfering signal, $i(t)$, and a noise term, $\eta(t)$. Each useful signal, $y_l(t)$ can be expressed as

$$y_l(t) = \sqrt{2C_l} d_l\left(t - \tau_{0,l}\right) c_l\left(t - \tau_{0,l}\right) \cos\left(2\pi(f_{RF} + f_{d,l})t + \varphi_{0,l}\right) \tag{2}$$

where

- C_l is the power of the lth useful signal;
- $d_l(\cdot)$ is the navigation message;
- $c_l(\cdot)$ is the lth pseudo-random sequence extracted from a family of quasi-orthogonal codes and used for spreading the signal spectrum
- $\tau_{0,l}$, $f_{d,l}$ and $\varphi_{0,l}$ are the delay, Doppler frequency and phase introduced by the communication channel
- f_{RF} is the centre frequency of the GNSS signal.

In (1), $i(t)$ can assume different forms depending on the type of interference source. For example, DME and pulsed pseudolite are characterized by quite different modulations. Despite such

differences, $i(t)$ can, in general, be modeled as

$$i(t) = i_c(t)p_s(t) \tag{3}$$

that is the product of two terms: $i_c(t)$ is a continuous component whereas $p_s(t)$ is a binary signal assuming values in $\{0, 1\}$ and defining a pulsing sequence. $p_s(t)$ defines the time instants when the interfering signal is effectively transmitted. When pseudolites are considered, $i_c(t)$ assumes the same form of (2). More specifically, having pseudolite signals with a structure similar to that of GNSS modulations is a choice common in the literature (Cobb; 1997; Stansell; 1986) and justified by fact that it implies minimal firmware changes for enabling pseudolite processing in current GNSS receivers. The pulsing scheme, $p_s(t)$, has been introduced as an effective technique for reducing interference problems (Cobb; 1997) on non-participating receivers.
The duty cycle

$$d = \lim_{T \to +\infty} \frac{1}{T} \int_{-T/2}^{T/2} p_s(t)dt \tag{4}$$

defines the average time during which the pulse interference is on.

Due to the quasi-orthogonality of the spreading codes, a GNSS receiver is able to process the L useful signals independently and (2) can be simplified as

$$r(t) = y(t) + i_c(t)p_s(t) + \eta(t) \tag{5}$$

where the indexes, l has been dropped for ease of notation.

Signal (5) is filtered and down-converted by the receiver front-end before being digitized. Digitization implies two different operations: sampling and amplitude quantization. In the following, sampling and quantization are considered separately. In addition, it is assumed that the signal is sampled without introducing significant distortions. After down-conversion and sampling, (5) becomes:

$$\begin{aligned} r_{IF}[n] &= y_{IF}(nT_s) + i_{c,IF}(nT_s)p_s(nT_s) + \eta_{IF}(nT_s) \\ &= y_{IF}[n] + i_{c,IF}[n]p_s[n] + \eta_{IF}[n] \end{aligned} \tag{6}$$

where the notation $x[n]$ is used to denote a discrete time sequence sampled at the frequency $f_s = \frac{1}{T_s}$. The index "IF" is used to denote a signal down-converted to an intermediate frequency, f_{IF}. In (6),

$$y_{IF}[n] = \sqrt{2C}d\left(nT_s - \tau_0\right)c\left(nT_s - \tau_0\right)\cos\left(2\pi\left(f_{IF} + f_0\right)nT_s + \varphi_0\right). \tag{7}$$

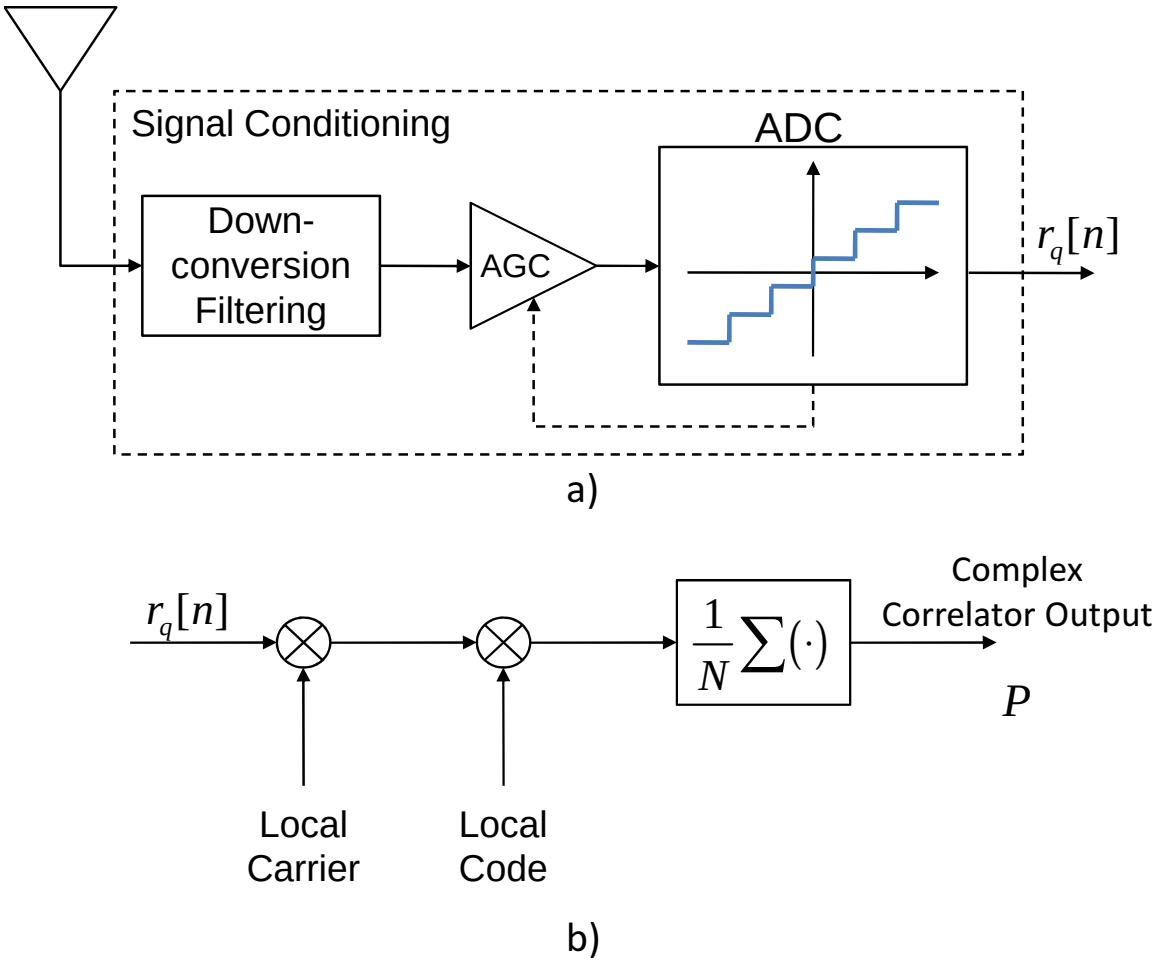

Fig. 1. Basic operations performed by a GNSS receiver. a) Signal conditioning: the RF analog signal is converted into an IF digital sequence. b) The correlation process.

The noise term, $\eta_{IF}[n]$, is assumed to be a white additive Gaussian noise with variance σ^2_{IF}. σ^2_{IF} depends on the filtering, down-conversion and sampling strategy applied by the receiver front-end and is given by $\sigma^2_{IF} = N_0 B_{IF}/2$ where B_{IF} is the front-end bandwidth and N_0 is the power spectral density of the input noise $\eta(t)$. The ratio between the carrier power, C, and the noise power spectral density, N_0, defines the Carrier-to-Noise density power ratio (C/N_0), one of the main signal quality indicators used in GNSS.

The amplitude quantization process is shown in the upper part of Fig. 1 and consists of a scaling, introduced by the AGC, and a mapping of the continuous values of $y_{IF}[n]$ into a finite discrete alphabet. This second operation is performed by the ADC. In this paper, ideal and very slow

AGC s are considered. Definitions of different AGC types are provided by Cobb (1997) and the considered cases are characterized by constant AGC gains. An ideal AGC ignores the interference pulse and provides a gain independent from the interference power. In the very slow case, the interference power impacts the selection of the gain that is fixed according to the total power measured by the AGC.

Under these conditions, the signal at the output of the ADC can be modeled as:

$$r_q[n] = Q_B\left[A_g\left(y_{IF}[n] + i_{c,IF}[n]p_s[n] + \eta_{IF}[n]\right)\right] \tag{8}$$

where $Q_B(\cdot)$ is the quantization function adopted by an ADC employing B bits for the signal representation. In a uniform quantizer, $Q_B(\cdot)$ is a symmetric stair-case function producing output values in the set $\left\{-2^B+1, -2^B+3, ..., -1, 1, ..., 2^B-3, 2^B-1\right\}$. A_g is the AGC gain. It is noted that depending on the number of levels used by the ADC and the interference power, several simplifications can be applied to (8). More specifically, two regimes can be considered (Borio et al.; 2011b):

- **small signal mode**, the power of the interference signal is small as compared to the noise variance. This allows one to develop a sort of linear approximation of the quantization function $Q_B(\cdot)$. $Q_B(\cdot)$ scales the signal components and introduces additional quantization noise;
- **saturation mode** the interference signal is so powerful to saturate the receiver ADC. Saturation implies that the pulsed interference, $i_{c,IF}[n]p_s[n]$, is always represented using the highest and lowest levels of the ADC, $\pm A_{max} = \pm 2^B - 1$.

Using the results derived in Borio et al. (2011a,b), it is possible to show that under the small signal regime, (8) can be approximated as

$$r_q[n] \approx \frac{a}{\sigma_{IF}}\left[y_{IF}[n] + i_{c,IF}[n]p_s[n]\right] + \eta_q[n] \tag{9}$$

where $\eta_q[n]$ is a zero mean random variable with variance

$$\text{Var}\left\{\eta_q[n]\right\} = b = 1 + 8\sum_{i=0}^{2^{B-1}-1} i\text{erfc}\left(\frac{i}{\sqrt{2}A_g\sigma_{IF}}\right). \tag{10}$$

where $\text{erfc}(\cdot)$ denotes the complementary error function (Abramowitz and Stegun; 1964). a is constant given by (Borio et al.; 2011a):

$$a = \sqrt{\frac{2}{\pi}}\left[1 + 2\sum_{i=1}^{2^{B-1}-1}\exp\left\{-\frac{i^2}{2A_g^2\sigma_{IF}^2}\right\}\right]. \tag{11}$$

It is noted that $\eta_q[n]$ is not Gaussian since it also accounts for the additional quantization noise. For large value of B, the probability distribution of $\eta_q[n]$ can be however approximated by a Gaussian probability density function (pdf).

Under the saturation mode, (8) becomes (Borio et al.; 2011b):

$$r_q[n] \approx Q_B\left[A_g(y_{IF}[n] + \eta_{IF}[n])\right](1 - p_s[n]) + A_{max}\text{sign}\left(i_{c,IF}[n]\right)p_s[n]. \tag{12}$$

where sign$(\cdot)$ is the sign function:

$$\text{sign}(x) = \begin{cases} -1 & x < 0 \\ 0 & x = 0 \\ 1 & x > 0 \end{cases}.$$

In this case, the quantization function is applied only to the signal and noise components. An approximation similar to that adopted for the small signal regime can then be applied to the quantized term in (12).

It is noted that there exists a transition regime modeling the passage between small signal and saturation modes. For such a regime, it is not possible to further simplify (8). In the following, (9) and (12) will be used as a basis for the theoretical analysis.

A. The Correlation Process

After signal conditioning, the sequence $r_q[n]$ is correlated with local replicas of the signal code and carrier. This process is shown in the lower part of Fig. 1 and a complex correlator output is computed as

$$P = \frac{1}{N}\sum_{n=0}^{N-1} r_q[n]c\left(nT_s - \tau\right)\exp\left\{-j2\pi(f_{IF} + f_d)nT_s - j\varphi\right\} \tag{13}$$

where τ, f_d and φ are the code delay, the Doppler frequency and the phase tested by the receiver. N is the number of samples used for computing a correlator output and $T_c = NT_s$ is the coherent integration time. It is noted that the computation of correlator outputs is essential for the proper functioning of a GNSS receiver and they are used both in acquisition and tracking (Kaplan and Hegarty; 2005), the main receiver operating modes. Thus, the quality of a GNSS signal can be defined after correlation as (Betz; 2000, 2001):

$$SNR_{out} = \max_{\tau, f_d, \varphi} \frac{\left|\text{E}\left\{P\right\}\right|^2}{\frac{1}{2}\text{Var}\left\{P\right\}} \tag{14}$$

where SNR_{out} is the coherent output Signal-to-Noise Ratio (SNR). The factor $1/2$ in (14) accounts for the fact that P is a complex quantity and only the variance of its real part is considered. The loss experienced at the correlator output, due to the presence of interference and after using mitigation techniques, is determined as the ratio between the measured SNR and the ideal coherent output SNR determined under ideal conditions.

III. Mitigation Techniques

In this section, IC and PB are briefly reviewed and their optimality discussed under different operating conditions.

It is noted that all the techniques considered in this paper are pre-correlation, i.e., they are applied on the signal $r_q[n]$ before the correlation process described in Section II-A. The interference is removed from $r_q[n]$ that can be then processed by the receiver.

Three pulsed interference mitigation techniques discussed in Section I are shown in Fig. 2 along with their relationships and possible configurations. Only IC and PB are considered in the following and the analysis of TF excision is left for future work.

Pulse interference mitigation techniques are strongly impacted by their knowledge of the interference signal. In this respect, PB and TF excision are special forms of IC when only a limited amount of information on the structure of the interference signal is available. Furthermore, even if the structure of the interference signal is known, some parameters still need to be estimated. For example, it is necessary to determine the pulse position, i.e., recover the pulsing scheme, $p_s[n]$. This can be achieved using different estimation techniques. In this paper, **thresholding** and **correlation-based** processing are considered. Thresholding implies the comparison of the input signal, $r_q[n]$, with a threshold, T. If, $|r[n]|$ is greater than T than the interference is declared present. Thus, pulse positions are determined through threshold passing. Correlation-based processing requires the correlation of the interference signal with a local replica of itself. The interference parameters are estimated as those that maximize the correlation with the local replica. This corresponds to a generalization of the matched filter.

Specific details on the different mitigation techniques are provided in the following.

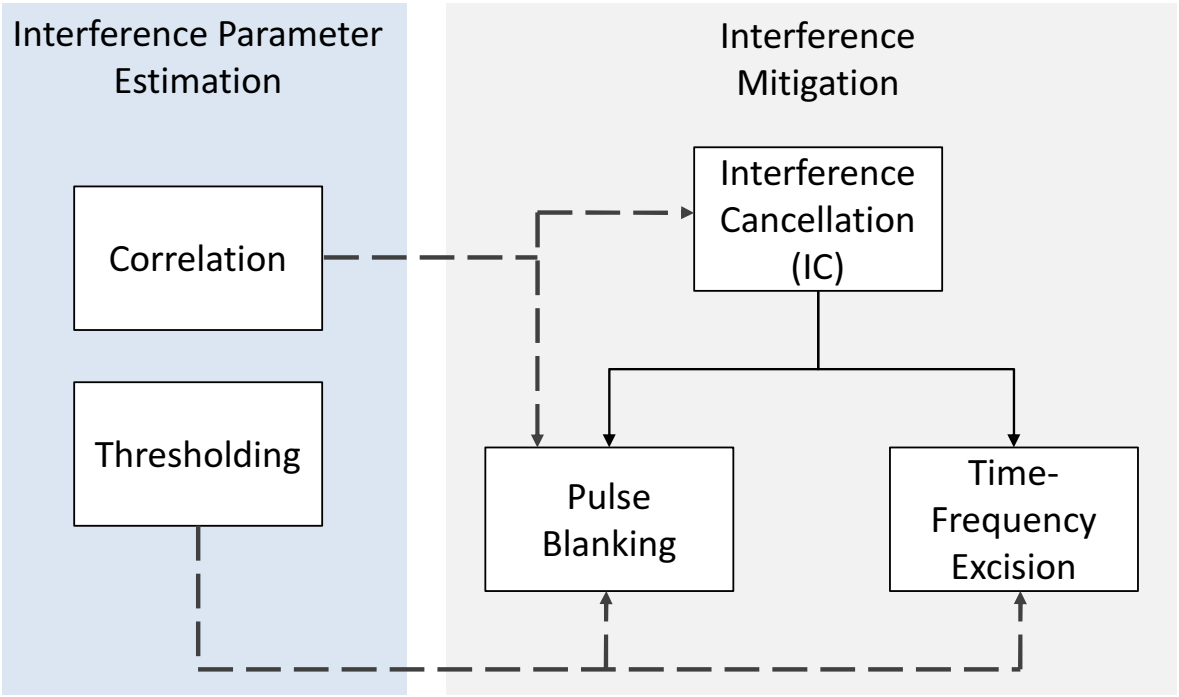

Fig. 2. Different pulsed interference mitigation techniques, their relationships and possible configurations.

A. *Interference Cancellation*

Consider signal model (9) and assume that the distribution of $\eta_q[n]$ can be effectively assumed Gaussian:

$$\eta_q[n] \sim \mathcal{N}(0, b). \tag{15}$$

In addition to this, assume that $i_{c,IF}[n]p_s[n]$ can be reconstructed from a finite number of parameters which are available to the receiver. This assumption is made to simplify the mathematical developments and will be removed in a second stage. When, the interfering signal is from a pulsed pseudolite, then $i_{c,IF}[n]$ can be expressed as (7) and the interference parameters are the amplitude, $\sqrt{2C_p}$, the code delay, τ_p, the Doppler frequency, $f_{d,p}$ and the phase, φ_p, of the pseudolite signal. The index 'p' is used to indicate quantities relative to the pseudolite signal.

When N samples of $r_q[n]$ are considered, it is possible to show that, under the previous hypotheses, the likelihood function to be maximized for determining the useful signal parameters,

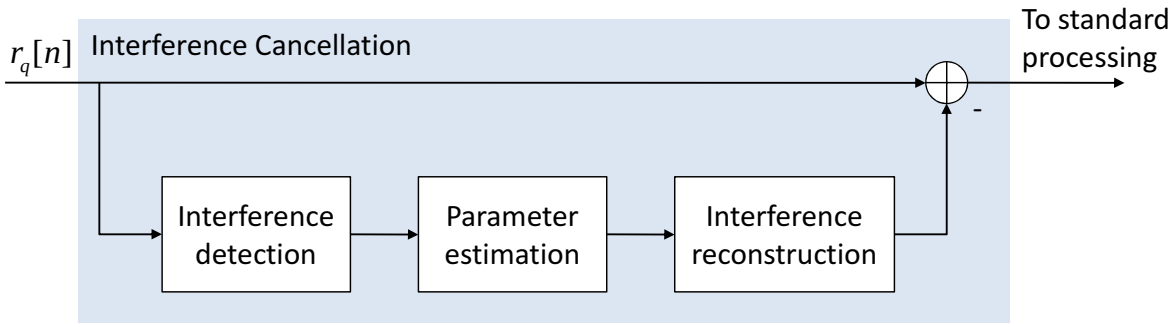

Fig. 3. Schematic representation of the IC process. The presence of the interfering signal is at first detected and its parameters estimated. The reconstructed interference component is then removed from the input signal, $r_q[n]$, that is passed to the GNSS receiver.

$\{\tau_0, f_0, \varphi_0\}$, is given by:

$$\Re\left\{\sum_{n=0}^{N-1}\underbrace{\left[r_q[n]-\frac{a}{\sigma_{IF}}i_{c,IF}[n]p_s[n]\right]}_{\substack{\text{interference}\\ \text{cancellation}}}\underbrace{c\left(nT_s-\tau\right)}_{\substack{\text{local}\\ \text{code}}}\underbrace{\exp\left\{-j2\pi\left(f_{IF}+f_d\right)nT_s-j\varphi\right\}}_{\text{local carrier}}\right\}. \quad (16)$$

The likelihood (16) is maximized when the parameters of the local carrier, φ and f_d, and local code, τ, match those of the incoming signal after interference removal. The processing described by (16) is analogous to standard correlation (13) where the interfering signal, $i_{c,IF}[n]p_s[n]$, has been at first removed.

IC is thus the optimum mitigation technique, in the Maximum Likelihood (ML) sense, when the impact of quantization can be neglected and the interference signal parameters are known. Since the interference parameters are seldom available an additional estimation block is required. More specifically, the interference presence needs to be detected and the interference parameters estimated as indicated in Fig. 3. The estimated interference parameters are used to reconstruct the interfering signal that is then subtracted from the input signal, $r_q[n]$.

If it were possible to completely remove the interference signal, $i_{c,IF}[n]p_s[n]$, then performance equal to that achieved in the absence of interference should be obtained. However, for low values of B, it is not possible to easily separate signal, interference and noise components. It is noted that the functional scheme depicted in Fig. 3 can still be used for low values of B, however the optimality of IC cannot be longer granted.

The effect of quantization on IC is analyzed in Section IV through simulations.

B. Pulse Blanking

PB consists of zeroing the samples containing the interference signal (Grabowski and Hegarty; 2002; Hegarty et al.; 2000) and can be derived by considering (12). Two types of random variables can be identified in (12):

- signal and noise samples, $Q_B\left(A_g(y_{IF}[n]+\eta_{IF}[n]\right)$, characterized by the probability mass function (pmf) $f_y\left(y|y_{IF}[n],\sigma_{IF}^2\right)$
- interference samples, $A_{max}\text{sign}\left(i_{c,IF}[n]\right)$, characterized by the pmf $f_i\left(i|i_{c,IF}[n]\right)$.

It is noted that although $f_y\left(y|y_{IF}[n],\sigma_{IF}^2\right)$ can have a complex expression depending on the quantization function, $Q_B(\cdot)$, it is a function of the signal samples and its parameters. $f_i\left(i|i_{c,IF}[n]\right)$ is a scaled Bernoulli pmf with mean depending on $i_{c,IF}[n]$. Moreover, due to ADC saturation, $f_i\left(i|i_{c,IF}[n]\right)$, is independent from the useful signal, $y_{IF}[n]$. All the samples of $r_q[n]$ are independent and the associated log-likelihood function can be written as

$$logL_{sat}\left(\tau,f_d,\varphi\right)=\sum_{n=0,p_s[n]=0}^{N-1}\log\left[f_y\left(y|y_{IF}[n],\sigma_{IF}^2\right)\right]+\sum_{n=0,p_s[n]=1}^{N-1}\log\left[f_i\left(i|i_{c,IF}[n]\right)\right] \quad (17)$$

where the position of the pulse is assumed known. In order to determine the signal parameter estimates, $\{\tau,f_d,\varphi\}$, the derivative of (17) has to be computed. Since the second summation in (17) is independent from $\{\tau,f_d,\varphi\}$, the derivative of this part of the likelihood is zeros. This implies that the ML estimator of $\{\tau_0,f_0,\varphi_0\}$ is independent from the interference samples that have to be excised. This operation is performed by PB that zeros the interference samples $A_{max}\text{sign}\left(i_{c,IF}[n]\right)$. PB is thus the optimal mitigation technique, in the ML sense, in the presence of ADC saturation.

Similarly to the IC case, (17) has been computed assuming the knowledge of the pulsing scheme, $p_s[n]$. This condition is rarely verified and an estimation block is required to determine $p_s[n]$. In this case, it is not necessary to recover all the parameters of the interfering signal, $i_{c,IF}[n]p_s[n]$, but only those of $p_s[n]$. A schematic representation of PB is provided in Fig. 4 (a): a detection block is used to recover the position of the interference pulses that are removed from the useful signal, $r_q[n]$. It is noted that PB can be though as a special case of IC where ADC saturation allows the separation between useful and interfering signal. The relationship between PB and IC is better illustrated in Fig. 4 (b). As for standard IC, the interference signal is detected and its parameters estimated. The reconstructed interference signal is then passed

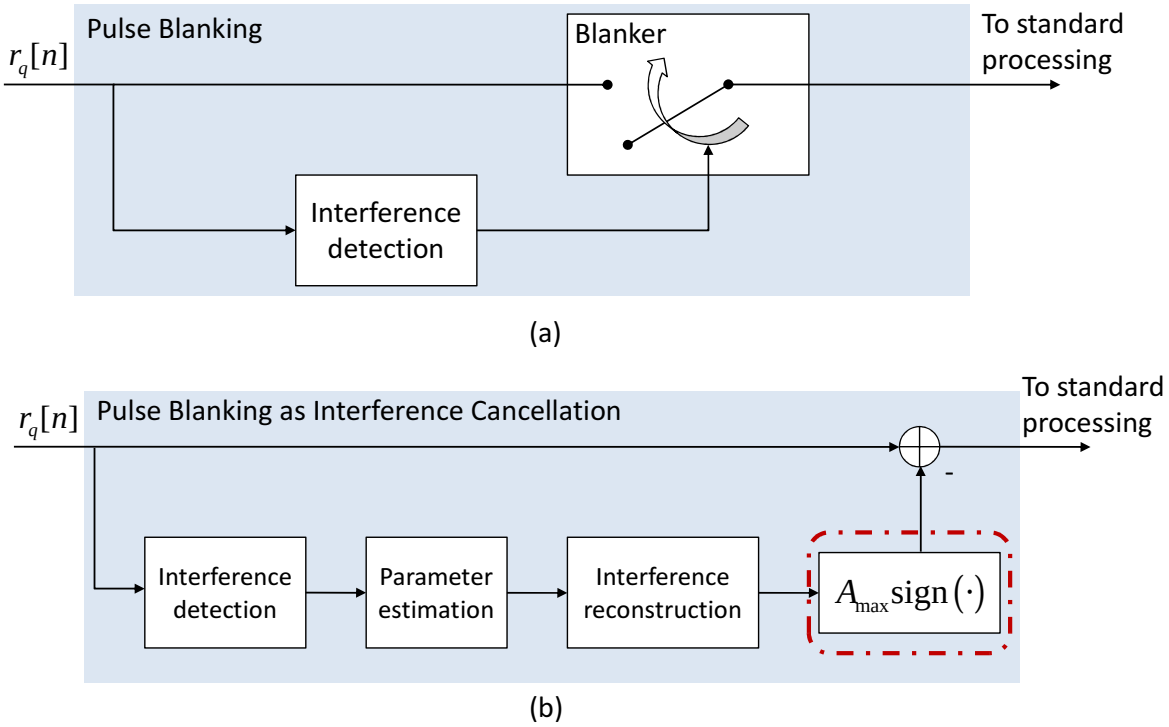

Fig. 4. (a) Schematic representation of the processing implemented by PB. (b) In the presence of ADC saturation, PB can be represented as a form of interference cancellation.

through the non-linear function $A_{max}\text{sign}(\cdot)$ that reproduces the effect of quantization in the presence of ADC saturation.

Several methods are available in the literature for determining the pulse position. In the following section, two situations are considered:

- **ideal blanking**: the pulse position is assumed known by the receiver. This could be the case of a participating pseudolite receiver which continuously tracks pseudolite signals and thus their pulse position is perfectly estimated
- **thresholding**: the pulse position is detected by comparing the input samples with a decision threshold, T.

C. PB SNR Loss in the Presence of Signal Conditioning

In this section, a theoretical model for the loss associated to pulse blanking in the presence of quantization is provided. In order to simplify the analysis, it is assumed that pulse interference

is saturating the ADC. For this case no results seem to be available in the literature whereas the loss experienced under the small signal regime can be obtained using the findings of Soualle et al. (2011) that neglected the impact of quantization and assumed a Gaussian noise term.
Before providing the loss model for PB using thresholding, some considerations are in order:

- if pulse positions were perfectly known then pulse interference would always be removed an the loss is given by the sum of two terms: the quantization loss and the excision loss. The quantization loss is given by (Borio; 2008):

$$L_q = \frac{2}{\pi} \frac{\left[1 + 2\sum_{i=1}^{2^{B-1}-1} \exp\left\{-\frac{i^2}{2A_g^2\sigma_{IF}^2}\right\}\right]^2}{1 + 8\sum_{i=1}^{2^{B-1}-1} i\text{erfc}\left(\frac{i}{\sqrt{2}A_g\sigma_{IF}}\right)} \tag{18}$$

  whereas the excision loss is equal to

$$L_{ex} = 1 - d \tag{19}$$

  and corresponds to an effective reduction in the integration time since dN samples are removed by sampling. The loss under ideal pulse synchronization conditions is thus given by

$$L_{ib} = L_q \cdot L_{ex}. \tag{20}$$

- when a single bit is used for quantization, it is not possible to determine the pulse position using a decision threshold. All the input samples are characterized by the same magnitude and thus is not possible to discriminate between useful and interfering signal.
- when PB is not implemented, the degradation due to pulse interference corresponds to the saturation loss derived by Borio et al. (2011b). It has been shown that receivers using a low number of bits have a natural immunity against pulsed interference. Thus, the saturation loss derived by Borio et al. (2011b) is used here as a comparison term.
- since PB is applied after quantization and the ADC produces values in the set

$$\left\{-2^B + 1, -2^B + 3, ..., -1, 1, ..., 2^B - 3, 2^B - 1\right\},$$

  the decision threshold, T, can assume only a limited number of values. Setting a threshold higher than $A_{max} = 2^B - 1$ is equivalent to disabling blanking whereas having a threshold lower than 1 causes the excision of all the samples. In addition to this, thresholds with

values between the same subsequent ADC output levels lead to the same pulse detection. For this reason, only thresholds in the set $\left\{2, 4, ..., 2^{B-1}\right\}$ are considered:

$$T \in \left\{2, 4, ..., 2^B - 2\right\}. \tag{21}$$

As for the ideal pulse synchronization case (denoted in the following as ideal blanking), the loss experienced when using thresholding can be expressed as the product of two terms:

$$L_{pb} = L_T \cdot L_{ex} \tag{22}$$

where L_T is the quantization loss experienced in the presence of thresholding. It is noted that this decomposition is only valid when the interference pulse is saturating the receiver ADC.
The loss, L_T, can then be computed using an approach similar to that adopted by Borio (2008) for computing the quantization loss in the absence of pulse blanking and is given by:

$$L_T = \frac{2}{\pi} \frac{\left[1 + 2\sum_{i=1}^{K} \exp\left\{-\frac{i^2}{2A_g^2\sigma_{IF}^2}\right\} - (2K+1)\exp\left\{-\frac{(K+1)^2}{2A_g^2\sigma_{IF}^2}\right\}\right]^2}{1 + 8\sum_{i=1}^{K} i\text{erfc}\left(\frac{i}{\sqrt{2}A_g\sigma_{IF}}\right) - (2K+1)^2\text{erfc}\left(\frac{K+1}{\sqrt{2}A_g\sigma_{IF}}\right)} \tag{23}$$

where

$$K = \left\lfloor \frac{T-1}{2} \right\rfloor \tag{24}$$

is the number of positive ADC levels not clipped by the pulse blanker.
The thresholding loss, L_T, is depicted in Fig. 5 as a function of the normalized AGC gain, $A_g\sigma_{IF}^2$, for the case of a 3 bit quantizer. The quantization loss (18) has also been provided for comparison purposes. From (23) and Fig. 5, it is possible to conclude that the optimal blanker threshold, T, is given by

$$T_{opt} = 2^B - 2 \tag{25}$$

i.e., only the samples equal to $\pm A_{max}$ are removed. This implies that only two levels of the quantization function, Q_B, are used for pulse detection whereas all the other levels are used for the useful signal representation. The optimal AGC level is also lower than that which should be used in the absence of interference. This result is explained by the fact that the useful signal and noise should be represented without using the highest/lowest levels of the quantization function. For AGC gain values closed to the optimum, L_T is close to L_q, the quantization loss.
The properties of the composite loss (22) are further analyzed in Fig. 6 where a duty cycle equal to 10% is considered. Three cases are considered: "Optimal Thresholding" refers to the

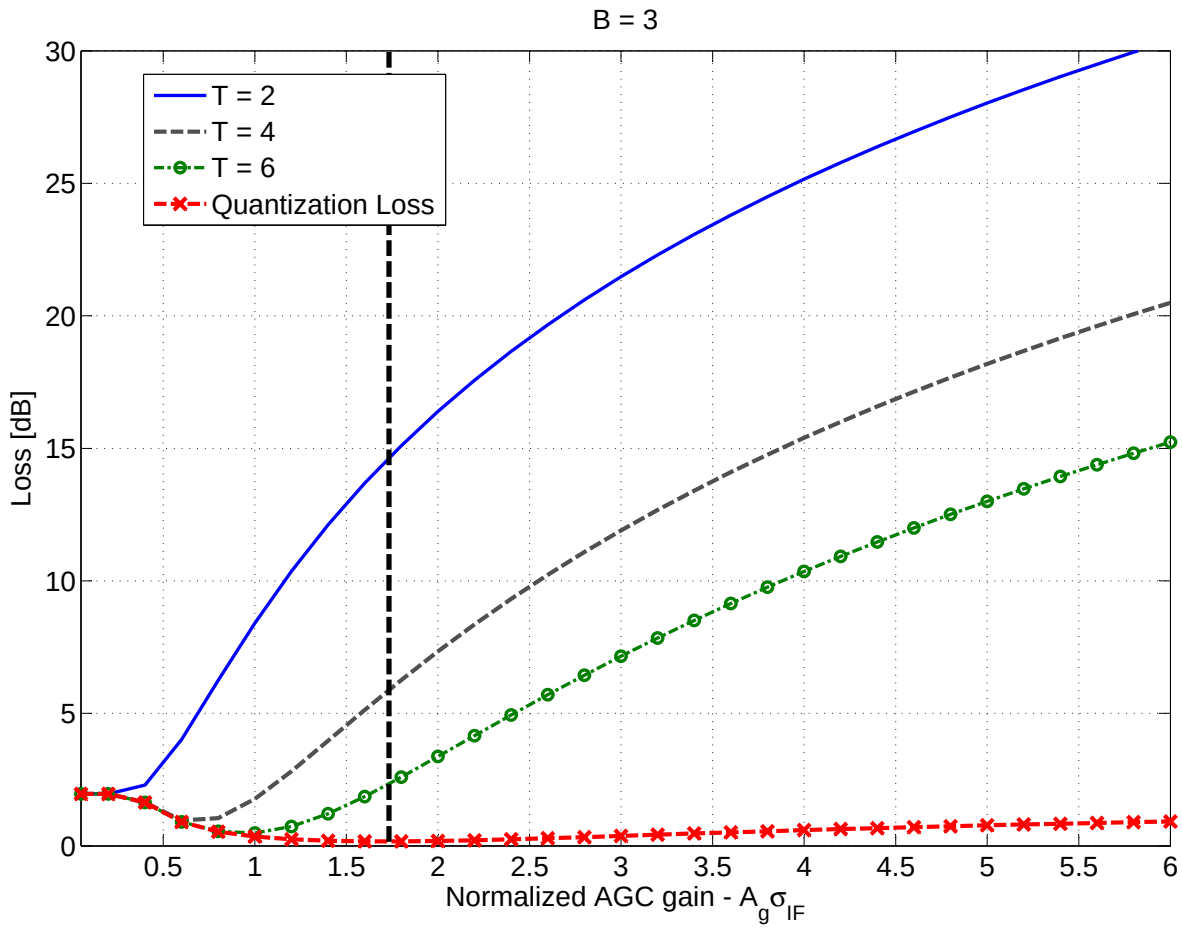

Fig. 5. Thresholding loss, L_T, for a 3 bit quantizer as a function of the normalized AGC gain, $A_g\sigma_{IF}^2$. The vertical line indicates the optimal AGC gain in the absence of interference.

case where L_T is computed for $T = T_{opt}$, the "No Blanking" curve has been obtained without applying any mitigation technique and "Ideal Blanking" corresponds to (20). The "No Blanking" case has been obtained using the saturation model proposed by Borio et al. (2011b).

From Fig. 6 it emerges that PB with thresholding is effective only if the AGC gain is properly set. In that case, the performance of thresholding are close to that achieved when the pulse position is known. It is also noted that the "Optimal Thresholding" and "No Blanking" curves have an intersection point. For an AGC gain greater than the intersection point, PB becomes ineffective and introduces additional signal losses.

These results are supported by simulations in Section IV.

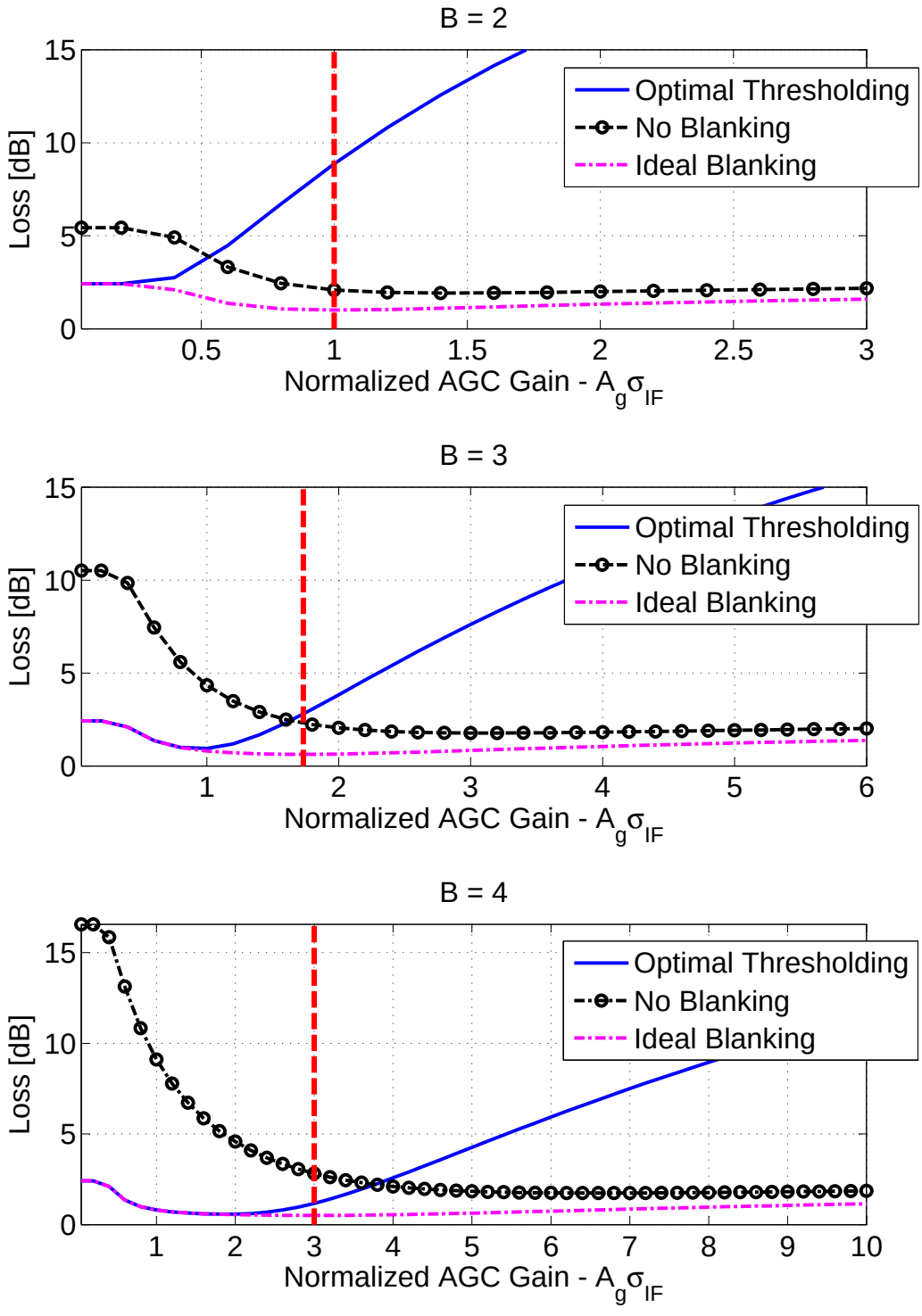

Fig. 6. Comparison of the SNR losses that a GNSS receiver would experience in the presence of pulsed interference for different number of bits and AGC gains. Vertical lines indicate the optimal AGC gain in the absence of interference. Pulse duty cycle, $d = 10\%$

TABLE I

PARAMETERS USED FOR THE EVALUATION OF PB AND IC MITIGATION TECHNIQUES THROUGH SIMULATIONS.

Parameter	Value
Coherent integration time, T_c	1 ms
Sampling frequency, f_s	5 MHz
Intermediate frequency, f_{IF}	1.42 MHz
C/N_0 of the GPS L1 system	45 dB-Hz
Number of Monte Carlo Simulation runs	10^5

IV. SIMULATION RESULTS

Simulation results giving insight into the behavior of IC and supporting the theoretical model developed for the computation of the SNR loss when PB is applied, are provided in this section.

At first, the case of a Global Positioning System (GPS) L1 Coarse/Acquisition (C/A) receiver, which applies IC, is considered. The GPS L1 C/A modulation was selected as a basis for the simulation of the useful and interfering pseudolite signals. The useful component was characterized by a C/N_0 of 45 dB-Hz. The pulsed pseudolite interference had a variable pulse duration given by the duty cycle, d and only one pseudolite pulse was generated for each useful signal code period. The power of the pseudolite interference signal was determined on the basis of the effective pseudolite C/N_0 and both small signal and saturation regimes were considered. The effective pseudolite C/N_0 is defined as

$$\frac{C_e}{N_0} = \frac{A_p^2 d}{2N_0}, \tag{26}$$

where A_p is the amplitude of the interference pulse. The effective C/N_0 accounts for the average interference power, which is reduced by a factor d. The main parameters employed in the simulation process are provided in Table I. The IC mitigation algorithm implemented in this work assumes the knowledge of the pseudolite signal position. For the signal reconstruction, the amplitude and phase of the quantized pseudolite component were estimated by correlating the quantized received signal with a local replica of the pseudolite interference. Subsequently, the locally generated pseudolite component was subtracted from the quantized received signal, as described in Section III-A.

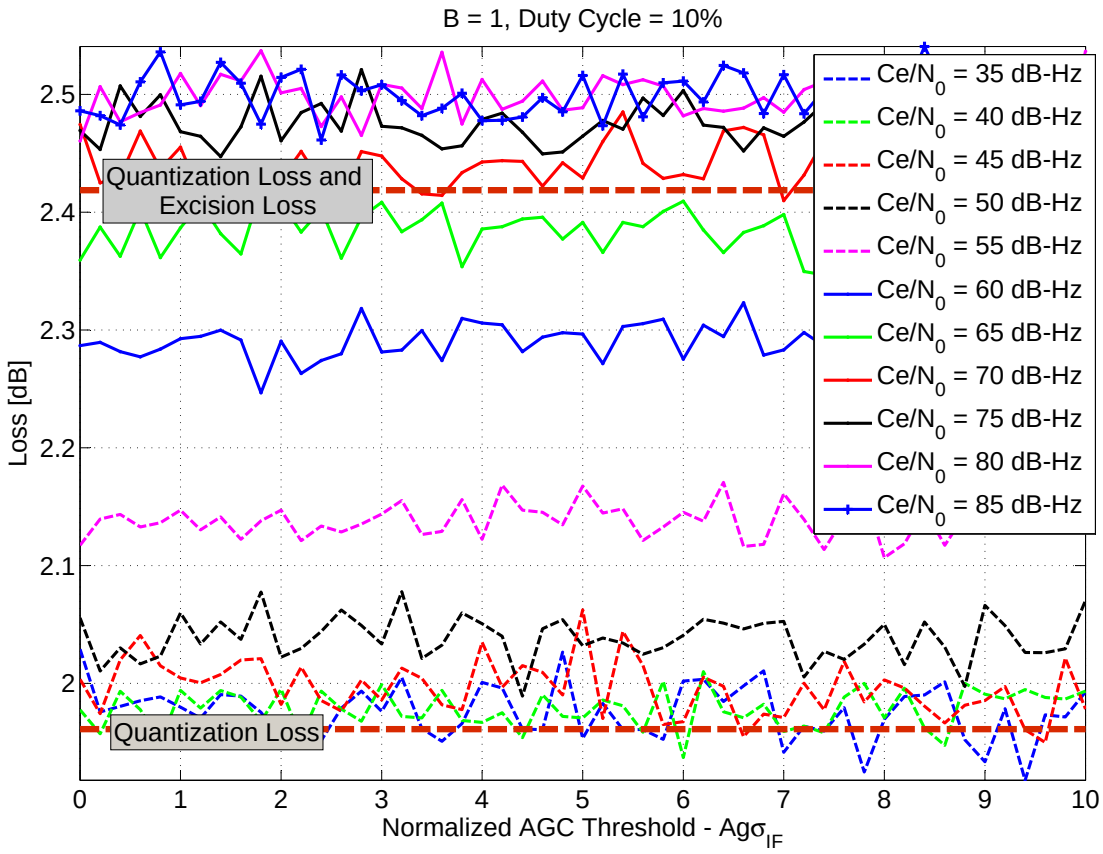

Fig. 7. SNR loss caused by pulsed interference and quantization as a function of the normalized AGC gain for different values of the effective pseudolite C/N_0. IC has been applied to mitigate the interference impact. $B = 1$, $d = 0.1$.

In the following, sample simulation results are provided where the cases $B = 1$ and $B = 4$ are considered. Similar results were obtained for other values of B.

The SNR loss, caused by pulsed interference and quantization after the IC, is plotted in Fig. 7, as a function of the normalized AGC gain, $A_g\sigma_{IF}$, for different values of effective pseudolite C/N_0. In this set of simulations, the number of quantized bits is equal to $B = 1$ and the duty cycle of the pulsed interferer is $d = 0.1$. As expected, the SNR loss is independent of the AGC gain, since only the sign of the input signal is retained by the quantizer and, therefore, the scaling introduced by the AGC has no effect on the computation of the SNR loss. Furthermore, for low values of effective C/N_0 ($C_e/N_0 < 55$ dB-Hz), where the small signal regime is assumed, IC effectively removes the pulsed interference from the input samples. In this case, a loss close to the sole quantization loss is achieved, as shown in Fig. 7. Conversely, for high values of

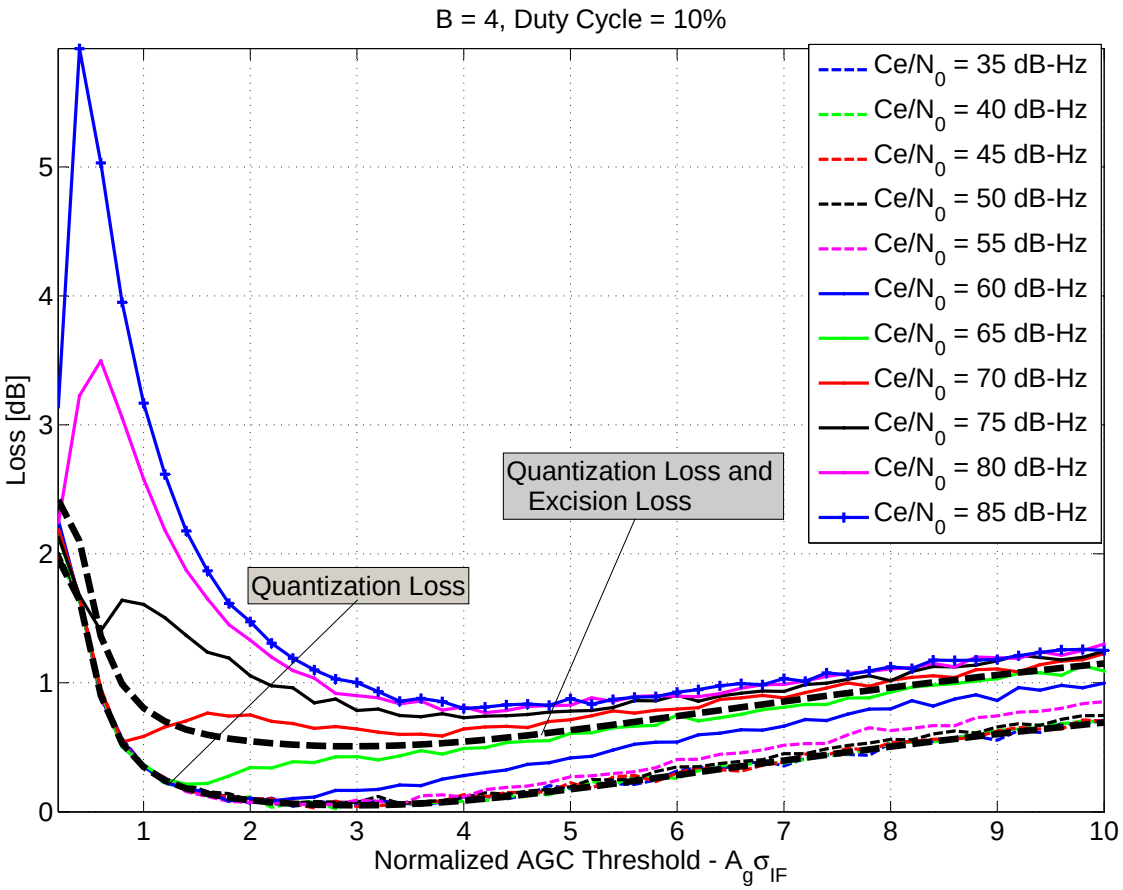

Fig. 8. SNR loss caused by pulsed interference and quantization as a function of the normalized AGC gain for different values of the effective pseudolite C/N_0. IC has been applied to mitigate the interference impact. $B = 4$, $d = 0.1$.

effective C/N_0 ($C_e/N_0 \geq 65$ dB-Hz), the pulse interference completely removes the useful and noise components (saturation mode), and IC is unable to reconstruct the useful signal. The SNR loss is slightly larger than the one given by the sum of the quantization and excision losses, as calculated in (20). In this case, IC is suboptimal and it is outperformed by ideal blanking. Simulation results considering a higher number of quantization bits, $B = 4$, are provided in Fig. 8. Conclusions similar to that derived for the $B = 1$ scenario can be reached. It is observed that, independent of the number of quantization bits, the IC technique is only optimal when pseudolite C_e/N_0 levels are low and interference does not saturate the quantizer (small signal regime).

Furthermore, simulations were carried out to support the validity of the theoretical frame-

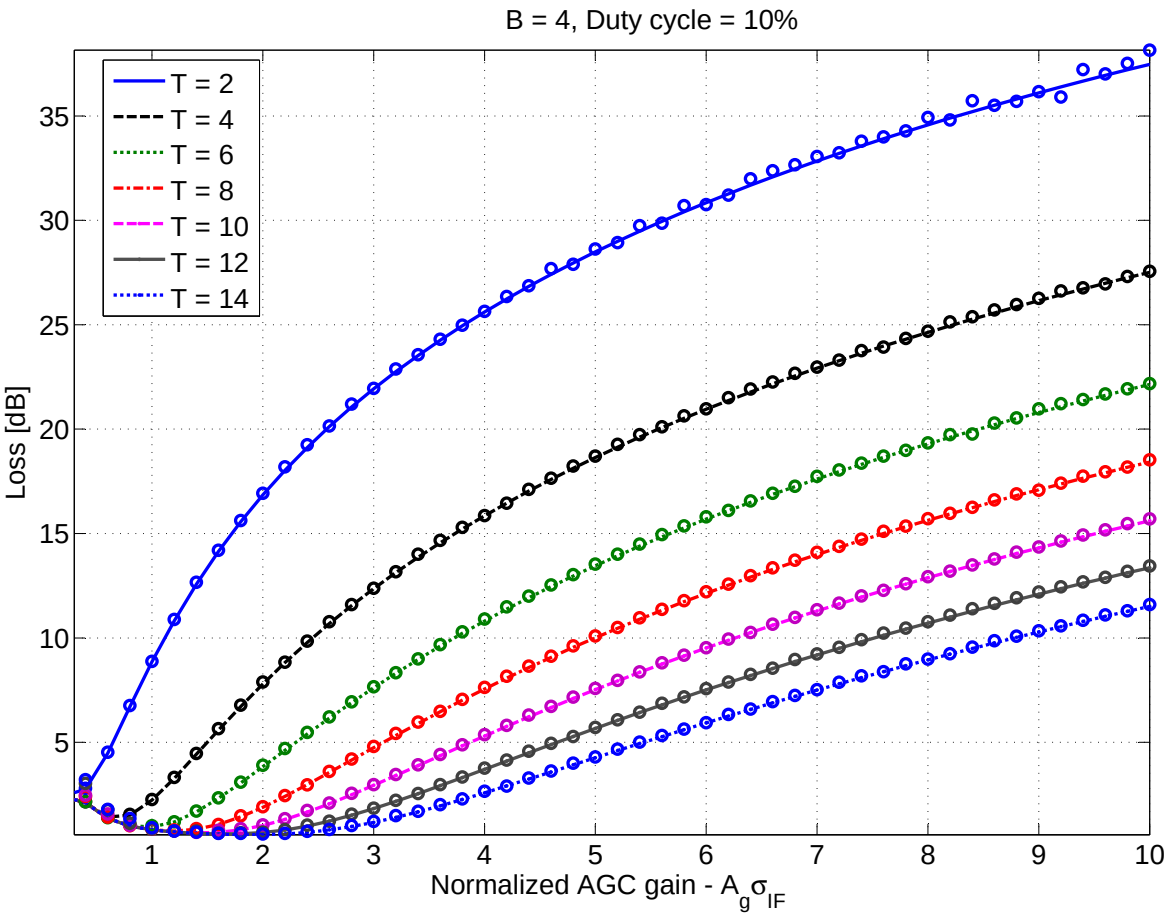

Fig. 9. Comparison between Monte Carlo and theoretical results. Circles are used to indicate simulation results.

work developed in Section III-C. The same parameters used for the IC analysis were used for simulating a GPS L1 receiver with PB and only the saturation regime was considered. Sample simulation results are shown in Fig. 9, where the SNR loss is depicted as a function of the normalized AGC gain and for different values of the threshold T. In this particular example, $B = 4$ and $d = 0.1$ were considered.

Simulation results are in good agreement with the theoretical findings supporting the validity of the theoretical framework developed for quantifying the loss in the presence of interference and PB.

Finally, a comparison between IC and PB in terms of SNR loss is provided in Fig. 10. In this scenario, the parameters $B = 3$ and $d = 0.1$ were considered. PB and IC mitigation techniques

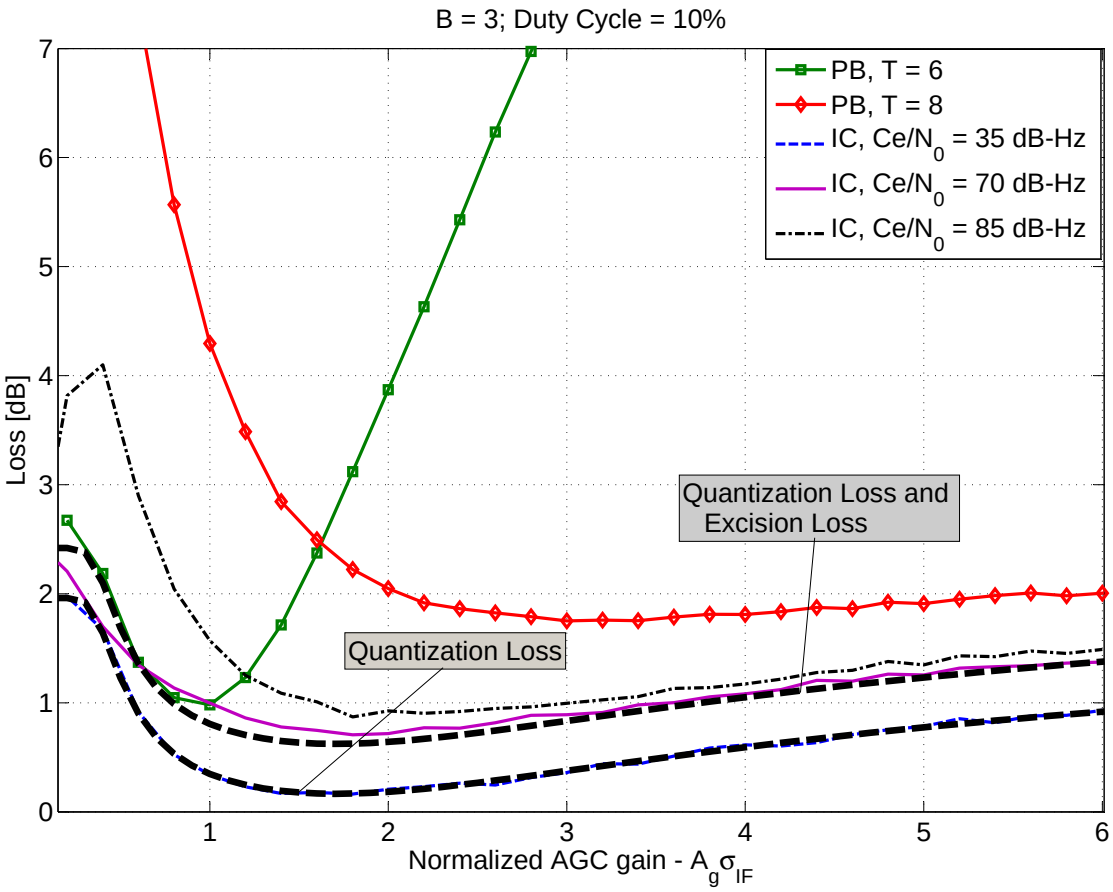

Fig. 10. Comparison between IC and PB techniques for $B = 3$ and $d = 0.1$ through Monte Carlo simulations. The PB thresholding method is implemented using $T = 6$ and $T = 8$, while the IC is applied to three different pulsed interference scenarios according to the pseudolite effective C/N_0.

have been used in this analysis. For PB method, the case of "Optimal Thresholding" given by (25) was considered, whereas IC was analyzed for three different interference scenarios: small signal ($C_e/N_0 = 35$ dB-Hz), saturation regime ($C_e/N_0 = 85$ dB-Hz) and an intermediate case ($C_e/N_0 = 70$ dB-Hz). In addition to this, the saturation loss obtained when no mitigation techniques are used, was included for comparison purposes. Simulation results show that the best performance in terms of SNR loss is obtained when the power of the pulsed interference is low (small signal mode) and IC is applied. However, only a marginal improvement (approximately 0.5 dB) is obtained by using IC with respect to PB with "Optimal thresholding". Since IC is more complex to implement than PB, a good compromise between performance and complexity is

achieved when PB is implemented with "Optimal Thresholding" and optimal AGC gain selection. It should be noted that PB with T_{opt} provides satisfactory performance if only the optimal AGC gain is selected. Significant SNR losses when the AGC gain is erroneously selected.

In saturation mode ($C_e/N_0 = 85$ dB-Hz), IC is no longer the optimal mitigation technique. In this case, it is observed from Fig. 10 that both "Ideal Blanking" and "Optimal Thresholding" with optimal AGC gain offer slightly better performance than IC. This result is in agreement with the theoretical findings developed in Section III.

V. Conclusions

In this paper, two pulsed interference mitigation techniques, IC and PB, have been analyzed in the presence of quantization and AGC scaling. IC is optimal in the absence of quantization and achieves performance close to that obtained in the absence of interference when the disturbing signal is not saturating the receiver front-end. This performance is achieved at the expenses of a high computational complexity since the algorithm requires the estimation of the interference parameters and the reconstruction of the disturbing signal. PB is less computationally demanding and is optimal in the presence of ADC saturation.

A novel theoretical framework for determining the SNR loss due to PB was developed. The theoretical findings provide an effective criterion for setting the PB parameters. More specifically, when thresholding is adopted for determining the position of the interference pulse, then only the lowest/highest level of the quantization function should be used for pulse excision. The AGC gain should be also reduced, with respect to the case of interference absence, to avoid the excision of the useful signal component.

Simulations were used for the analysis of the considered mitigation techniques under different operating conditions. The results confirm the optimality of IC in the absence of saturation and support the theoretical findings obtained for PB.

From the comparison between IC and PB, it emerges that, despite the superiority of IC for a wide range of interference power levels, the performance improvement with respect to PB is marginal when its parameters (AGC gain and blanking threshold) are properly set. The theoretical and simulation results obtained in the paper, provide insight on the behavior of the aforementioned mitigation techniques and represent an effective tool for their design and integration in an advanced GNSS receiver.

REFERENCES

Abramowitz, M. and Stegun, I. A. (1964). *Handbook of Mathematical Functions with Formulas, Graphs, and Mathematical Tables*, Dover, New York.

Betz, J. W. (2000). Effect of narrowband interference on GPS code tracking accuracy, *Proc. of ION National Technical Meeting*, Anaheim, CA, pp. 16–27.

Betz, J. W. (2001). Effect of partial-band interference on receiver estimation of C/N_0, *Proc. of the 2001 National Technical Meeting of The Institute of Navigation*, Long Beach, CA, pp. 817 – 828.

Borio, D. (2008). *A statistical theory for GNSS signal acquisition*, Phd thesis, Politecnico di Torino.

Borio, D. and Fortuny, J. (2010). Impact of pseudolite signals on non-participating GPS receivers: Compatibility analysis for commercial receivers, *Technical report*, EC Joint Reseach Centre.

Borio, D., O'Driscoll, C. and Fortuny, J. (2011a). Impact of pseudolite signals on non participating GNSS receivers, *Proc. of the European Navigation Conference*, London, UK, pp. 1–11.

Borio, D., O'Driscoll, C. and Fortuny, J. (2011b). Impact of pseudolite signals on non-participating GNSS receivers. modelling receiver losses, *Technical report*, EC Joint Reseach Centre.

Cobb, S. H. (1997). *GPS pseudolites: Theory, Design and Applications*, Phd thesis, Stanford University.

Gao, G. X. (2007). DME/TACAN interference and its mitigation in L5/E5 bands, *Proc. of the ION/GNSS*, Fort Worth, TX, pp. 1191–1200.

Grabowski, J. and Hegarty, C. (2002). Characterization of l5 receiver performance using digital pulse blanking, *Proc. of the ION GPS*, Portland, OR, pp. 1630–1635.

Hegarty, C., Dierendonck, A. J. V., Bobyn, D., Tran, M. and Grabowski, J. (2000). Suppression of pulsed interference through blanking, *Proc. of the IAIN World Congress and the Annual Meeting of The Institute of Navigation AM/ION*, San Diego, CA, pp. 399–408.

Kaplan, E. D. and Hegarty, C. (eds) (2005). *Understanding GPS: Principles and Applications*, 2nd edn, Artech House Publishers.

Madhani, P., Axelrad, P., Krumvieda, K. and Thomas, J. (2003). Application of successive

interference cancellation to the gps pseudolite near-far problem, *IEEE Trans. Aerosp. Electron. Syst.* **39**(2): 481 – 488.

Nava, S. A. and Scarafia, S. (2006). *Analysis and Simulations of Mitigation Techniques for Pulsed Interferers on GNSS Signals*, PhD thesis, Politecnico di Torino.

Paonni, M., Jang, J., Eissfeller, B., Wallner, S., J., J. R., Samson and Fernandez, F. (2010). Innovative interference mitigation approaches: Analytical analysis, implementation and validation, *ESA Workshop on Satellite Navigation Technologies and European Workshop on GNSS Signals and Signal Processing (NAVITEC)*, pp. 1 –8.

Soualle, F., Cattenoz, M., Giger, K. and Zecha, C. (2011). Improved analytical models of SNIR degradation in presence of pulsed signals and impact of code-pulse synchrony, *Proc. of the Fifth European Workshop on GNSS Signals and Signal Processing*, Institut Aéronautique et Spatial (IAS), Toulouse, France.

Stansell, T. A. (1986). RTCM SC-104 recommended pseudolite signal specification, *NAVIGATION: Journal of The Institute of Navigation* **33**(1): 42–59.